Characterization and sorption properties of low pH cements

Naila Ait Mouheb[1*], Vanessa Montoya[1], Dieter Schild[1], Eva Soballa[1], Christian Adam[1], Frank Geyer[1], Thorsten Schäfer[1]

[1] KIT, Institut für Nukleare Entsorgung (DE)

* Corresponding author: naila.ait-mouheb@kit.edu

Abstract

Characterization of three low pH cement pastes, including the description of their sorption properties for tritiated water (HTO), $^{36}Cl^-$ and $^{129}I^-$ is described in this work. SEM-EDX and NMR analyses show that after 90 days of hydration, the main hydrated phases are C-S-H and C-A-S-H gels with a Ca:Si ratio between 0.8 - 1.0 and a Al:Si ratio of 0.05. TG-DSC and XRD indicate the presence of calcite in the mixtures where limestone filler has been used. Additional techniques were used to identify minor hydrated solid phases like ettringite (i.e., XRD and solid state NMR). Porosity and pore size distribution was characterized by MIP observing that the size of the pores in the hydrated cement phases varies from the micro to the nanoscale. Uptake studies of HTO, $^{36}Cl^-$ and $^{129}I^-$ from batch sorption experiments indicate very weak sorption ($K_d < 0.40 \pm 0.13$ L/kg) for the 3 selected radionuclides. The uptake process of $^{36}Cl^-$ and $^{129}I^-$ is probably associated with surface processes in the C-S-H and C-A-S-H phases with competition for sorption sites, between them. In the case of HTO, isotopic exchange with the interlayer water of the C-S-H and the C-A-S-H seems to be the main uptake process.

Introduction

The deep geological repository concept of nuclear waste is based on the confinement of the radioactive waste over a long period of time by multiple barriers. Many of the concepts developed internationally use concrete and clay as confinement barriers (ANDRA, 2005; ENRESA, 1995). The different barriers are not in geochemical equilibrium and during the prolonged period of post disposal, cementitious material will undergo alterations, possibly changing the chemical and physical properties of this barrier. One important process that could reduce the durability of a concrete barrier is the leaching / degradation of the solid especially at the cement / clay interface due to the contact of clay pore water with the cementitious material. In order to minimize the interaction between the "classical" cement materials and the bentonite porewater (pH ~ 7.5) low pH cements were developed within the nuclear waste disposal context in the late 90's.

The main characteristic of these low pH cements is the absence of portlandite as hydrated solid phase, which reduces the pore water pH to ~ 11 compared to the "classical" cements (pH ≥ 12). Thus, to obtain 'low pH' cement, the clinker content in the binder is substituted for supplementary materials like silica fume or fly ashes (Coumes et al., 2006). From a chemical point of view the Ca/Si ratio composition in the hydrated low pH cement is less than 1.0 and C-S-H phases are the main solids present.

In the framework of the CEBAMA project, KIT-INE is studying the interaction between low pH cement materials and bentonite pore water, assessing the impact of mineralogical and microstructural modifications on transport properties and its effect on the mobility of radionuclides. To evaluate time dependent changes on

transport properties and mineralogical composition in the geochemical perturbed system, it is crucial to have a detailed physicochemical characterization of the cementitious starting materials under equilibrium conditions. The objective of this contribution is to complete the characterization of the cement samples started in the first year of the project (Ait Mouheb et al., 2017) using X-ray diffraction (XRD), thermogravimetric - differential thermal analysis (TG-DTA), ^{29}Si and ^{27}Al magic angle spinning nuclear magnetic resonance spectroscopy (^{29}Si and ^{27}Al MAS NMR), scanning electron microscopy - energy dispersive X-ray spectroscopy (SEM-EDX) and mercury intrusion porosimetry (MIP). In addition, sorption properties of the low pH cements to HTO, $^{36}Cl^-$ and $^{129}I^-$ at tracer concentrations have been investigated.

Materials

Cement Samples preparation

Three different low pH cement pastes (MIX 3C, 3D and 3E) consisting either of binary or ternary binder composition with sulphate resistant Portland cement (CEM I 52.5N SR, from Lafarge), silica fume (microsilica ELKEM 940U) and limestone filler ($CaCO_3$) have been prepared and described in Ait Mouheb (2017) (see Table 1). An inorganic superplasticizer (SioxX®) was used to achieve good workability in the MIX 3C.

The mixtures have been hydrated with de-ionised water using a water/binder ratio (w/b) = 0.6 and the samples have been cured in a chamber at 98% relative humidity (RH) and 21 ± 2°C during 90 days.

Table 1: *Composition (w.w.%) of the solid mixtures proportions used in this work.*

	MIX 3C (%)	MIX 3D (%)	MIX 3E (%)
OPC (CEM I 52.5 N)	39	40	50
Silica fume (ELKEM 940U)	39	40	50
Limestone filler	19	20	-
Superplasticizer (SioxX)	3	-	-

Low pH artificial cement water (ACW)

A low pH artificial cement pore water (ACW) was prepared by dissolving: 645.5 mg KOH, 639.9 mg Na_2SO_4, 363.7 mg $Na_2Si_3O_7$, 617.8 mg $CaCl_2{:}2H_2O$ and 295.9 mg $Ca(OH)_2$ in 2 L Milli-Q water. Then, 1.2 mg $CaCO_3$ and 295.9 mg $Ca(OH)_2$ were added. The solution was shaken for one week inside of a glove box filled with Ar. The pH was adjusted with 180 mL of H_2SO_4 (0.04 M) at pH = 11.0. Finally, the ACW is centrifuged (Heraeus Megafuge 2.0R) for 30 min. Later, the supernatant was filtrated by PVDF membrane with a pore size of 0.22 µm. The composition of the synthetized water is specified in Table 2.

Table 2: *Chemical composition of the artificial cement water (pH = 11.01) analysed by ICP-OES and ion chromatography.*

Element	Concentration (M)	Element	Concentration (M)
Na	$5.87 \cdot 10^{-3}$	**$CO_3^{(*)}$**	$2.76 \cdot 10^{-6}$
K	$3.76 \cdot 10^{-3}$	**S(VI)**	$5.75 \cdot 10^{-3}$
Ca	$3.56 \cdot 10^{-3}$	**Cl**	$3.84 \cdot 10^{-3}$
Si	$1.46 \cdot 10^{-3}$		

(*) Total concentration

HTO, ^{36}Cl- and ^{129}I- stock solutions

A stock solution containing HTO and ^{36}Cl was prepared by adding 450 µL of HTO solution ($1.01 \cdot 10^7$ Bq/mL) and 538.9 µL of ^{36}Cl solution ($7.42 \cdot 10^5$ Bq/mL) in 2 L of low pH artificial cement water. The concentration of the radiotracers were [HTO] = $1.86 \cdot 10^{-9}$ M and [^{36}Cl] = $4.55 \cdot 10^{-6}$ M. A separate stock solution containing ^{129}I was prepared by adding 270.3 µL of ^{129}I ($3.7 \cdot 10^5$ Bq/mL) in 2 L of low pH artificial cement water ([^{129}I] = $5.93 \cdot 10^{-5}$ M).

Methods

Analytic techniques used for cement characterization

Different techniques (SEM-EDX, XRD, TG-DSC) were used to characterize the three mixtures as described in Ait Mouheb et al. (2017). Additionally, ^{29}Si and ^{27}Al magic angle spinning nuclear magnetic resonance spectroscopy (^{29}Si and ^{27}Al MAS NMR) have been used in this contribution. The ^{29}Si and ^{27}Al MAS NMR spectra were acquired on a Bruker Avance III 400 wide-bore spectrometer. The instrument operates at 104.28 MHz for ^{27}Al and 79.50 MHz for ^{29}Si. The samples were placed in a disposable Kel-F container and then inserted into a standard ZrO_2 rotor. All experiments were carried out at room temperature with a magic angle spinning frequency of 15 kHz.

Spectra were recorded using standard Bruker pulse sequences. For iron-free samples, the FID (free induction decay) was recorded with 32 k data points and zero filling to 64 k was applied. For ^{27}Al, after a 90° excitation pulse, 512 scans with a relaxation delay of 500 ms were acquired. For ^{29}Si, the excitation pulse angle was 30° and at least 4 k scans with a delay of 15 - 20 s were used. The paramagnetism of iron-containing samples required different experimental conditions. Only 8k - 16k data points were sampled. For ^{27}Al, 8 k scans with a delay of 250 ms were performed; for ^{29}Si, 64 k scans were accumulated and the delay reduced to 500 ms. For the processing, no zero-filling was applied, and multiplication with Gauss functions was used (5 - 10 Hz line broadening).

The observed ^{29}Si resonances were analysed using the Q_n(mAl) classification, where a Si tetrahedron is connected to n Si tetrahedral with n varying from 0 to 4 and m is the number of neighbouring AlO_4 tetrahedrons.

Kinetic batch sorption experiments

The sorption studies of HTO, ^{36}Cl and ^{129}I were carried out by duplicate in a glove box under a controlled Ar atmosphere (O_2 and CO_2 concentrations < 5 ppm). 2.67 grams of each cement sample (mix 3C, 3D and 3E) were added in different polystyrene tubes. Then, 20 mL of the prepared stock solution containing HTO and $^{36}Cl^-$ were added obtaining a suspension with solid-liquid ratio of 133 g/L. The same procedure was used to do the sorption experiments with $^{129}I^-$.

The suspensions were mixed continuously for 1 day to 30 days using roller mixers. After the selected time, mixing was stopped and the suspension is filtrated using Polyvinylidene fluoride filters (PVDF) with a pore size of 0.45 µm inside of the glovebox. Subsequently, the supernatant was measured by liquid scintillation spectrometry (LSC) in order to determine the activities of each radionuclide. Results are expressed as distribution ratio R_d (Eq. 1) which corresponds to the ratio S/C, where S is the amount of tracer adsorbed onto the unit mass of the solid phase, and C is the amount of tracer per unit volume of solution.

$$R_d = \frac{Quantity\ of\ a\ radionuclide\ sorbed\ per\ unit\ mass\ cement}{Equilibrium\ concentration\ of\ the\ radionuclide\ in\ pore\ water}\ \left[\frac{L}{kg}\right] \qquad \textbf{\textit{Eq. 1}}$$

Results and discussion

Characterization of the cement samples

X-Ray diffraction after 90 days of hydration

According to Ait Mouhed et al. (2017) and based on XRD analysis the three synthesized mixtures were highly hydrated after 90 days of hydration not observing any phase of the clinker in the difractogram. The only clear identifiable crystalline solid phase was calcite for the samples 3C and 3D. C-S-H phases could not be detected in any of the samples probably due to its low crystallinity.

The Rietveld refinement using the Topas Academic v4.2 software was applied to quantify the crystalline and amorphous phase composition of the three mixtures. The amorphous phases were hypothesized to be C-S-H phases and are present as major phases in all the samples: 82% for the samples 3C and 3D and 92% for 3E (see Figure 1). Additionally, calcite is present as 12% in sample 3C and 3D and in less of 2% in 3E. Small amounts (< 6%) of crystalline C-S-H phases (Tobermorite type) was quantified as well (see Figure 3).

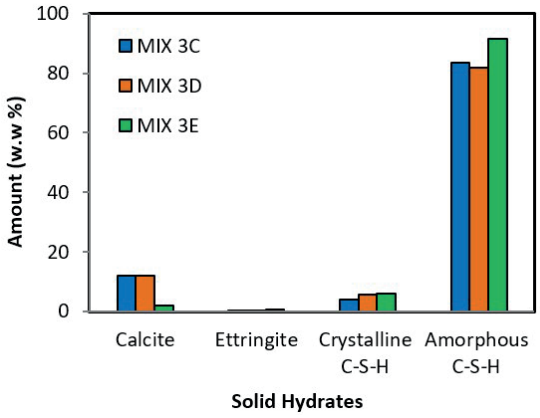

Figure 1: *Quantitative Rietveld phase analysis of the three samples: MIX 3C (in blue), MIX 3D (in orange) and MIX 3E (in green).*

TG - DSC after 90 days of hydration

Thermogravimetric analysis (TG) can give quantitative information of the different phases present in the samples by measuring the temperature dependent mass loss (wt.%). In addition, differential scanning calorimetry (DSC) measures the heat difference related to enthalpy changes caused by loss of water or CO_2 or recrystallization reactions. In Figure 2, the mass loss (%) and the differential scanning calorimetry (DSC) data of the three samples are presented. The interpretation of the TG analyses (Ait Mouheb et al., 2017) revealed C-S-H, ettringite and calcite phases. The mass loss at 820°C, not discussed in the previous contribution, is attributed to the decomposition of C-S-H to wollastonite ($CaSiO_3$) by dehydroxylation (Beaudoin et al., 1990).

Additionally, thermogravimetric analysis has been applied to measure the water bound in cement samples corresponding to the interlayer water in C-S-H hydrate, structural water in ettringite, and adsorbed water, except water in micropores or in larger pores. The amount of water bound in the 3 samples was calculated according to the method described in Lothenbach et al. (2012) which consists of measuring the total mass loss up to 500°C of the 3 samples, after exchange with isopropanol and drying the samples at 40°C. An average value of 28.17 ± 1.70 wt.% has been calculated for the 3 studied mixtures.

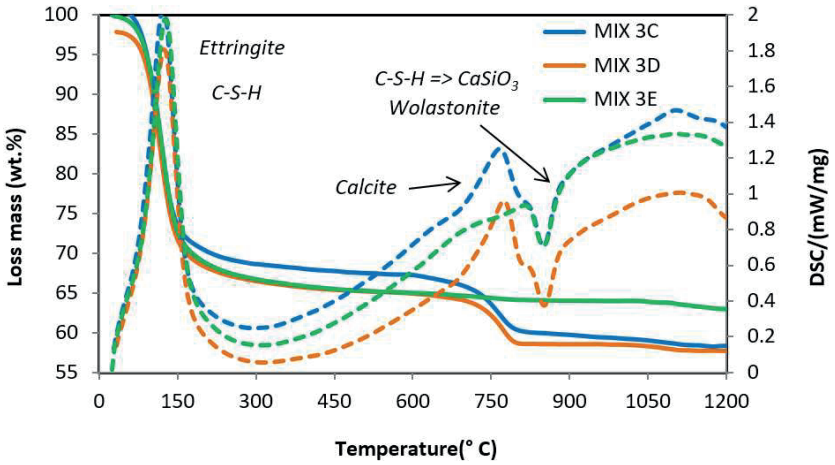

Figure 2: *Mass loss (wt.%) recorded by TG analysis (solid line) and differential scanning calorimetry (DSC) (dotted line) for MIX 3C, 3D and 3E (after 90 days of hydration).*

4.1.3 SEM-EDX analyses after 90 days of hydration

The three pastes were analyzed by SEM-EDX to observe the morphology and chemical composition of the different hydrated phases (Ait Mouheb et al., 2017).

In order to determine the different phases and the Ca/Si ratios of the C-S-H phase elemental maps of the surface were conducted by SEM-EDX. Sixty different spots have been investigated to determine the atomic ratio of Ca, Al, Si, C, Fe, S, Na, Mg and K. In Figure 3, the data analyses for the 3 samples is depicted by the plot of Al/Ca versus Si/Ca atomic ratios analyzed at several points of the mix 3C, 3D and 3E samples. According to Ait Mouheb et al. (2017) and Figure 3, the analyses show that mix 3C, 3D and 3E are composed essentially by C-S-H phases with Ca/Si ratios in the range of 0.6 to 0.8.

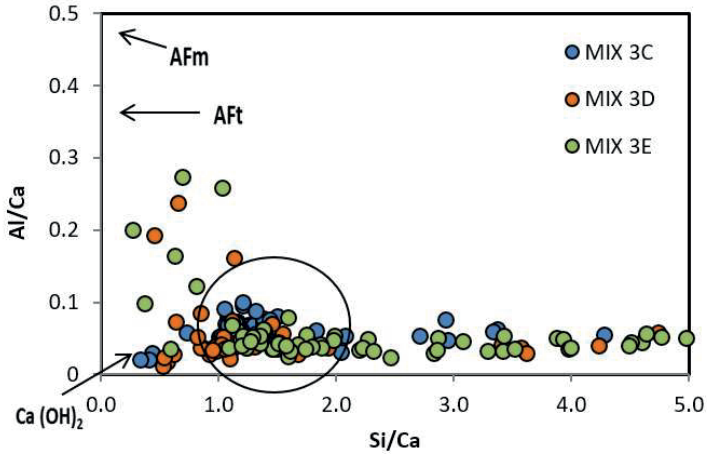

Figure 3: *Al/Ca versus Si/Ca atomic ratios for different microanalyses spots of the mixture 3C, 3D and 3E after 90 days of hydration.*

Finally, to complete the interpretation of the data and to show the heterogeneity of the sample, elemental maps of calcium (yellow), silicon (red) and aluminium (blue) and the measurement of the Ca/Si ratio by SEM-EDX on all samples is depicted in Figure 4. The atom percentage increases with the intensity of the colour in the mix 3C, 3D and 3E (maximum silica content 35%, 29% and 59%, calcium 26%, 22% and 24%, aluminum 13% - 5% and

10%) respectively, whereas black areas represent pores or fractures. Superposition of the calcium, silica and aluminum content as RGB image allows to clearly distinguish three different zones (see Figure 4). The orange color in the RGB images represents areas of C-S-H phase predominance, whereas purple - blue colors are probably attributed to non-reacted OPC and the red color represents areas of non-reacted silica fume.

Figure 4 also shows the spatial resolved element distribution of iron, aluminium and sulphate. Superposition of these elements indicate that iron is mainly present as a pure solid phase, probably mainly as ferrite or hydroxide not detected by XRD. Aluminium is also associated with sulphate, probably as ettringite.

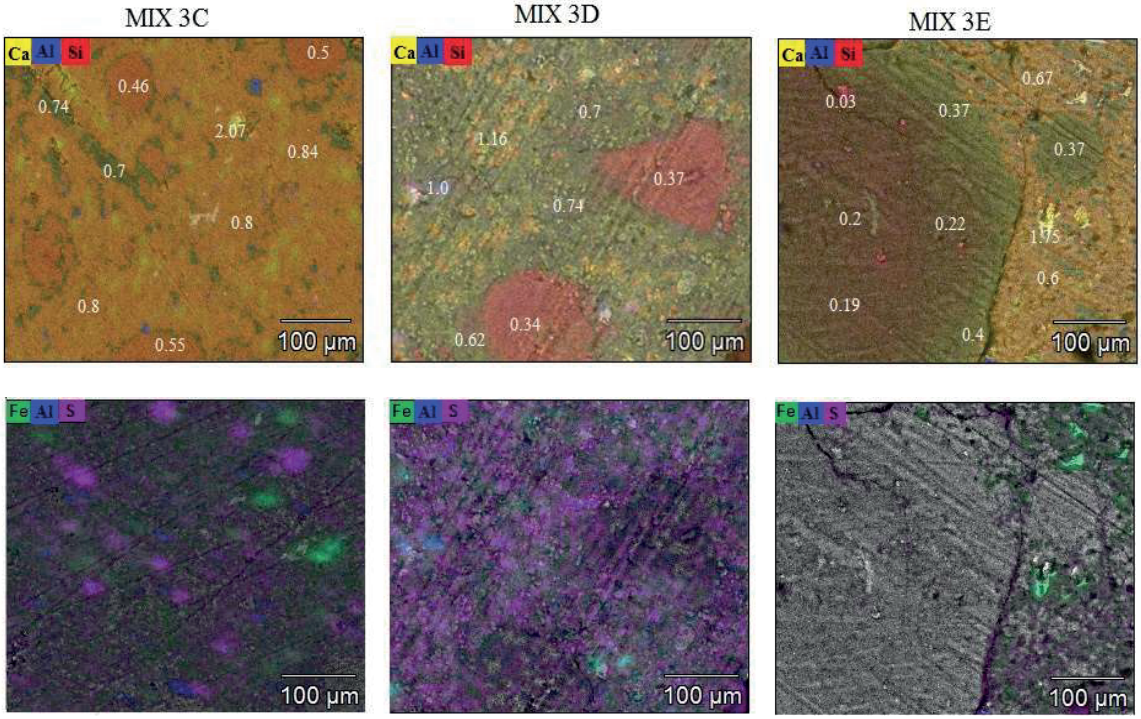

Figure 4: *SEM-EDX elemental maps of calcium (yellow), silicon (red)and aluminium (blue) together with local Ca/Si ratios of samples 3C, 3D and 3E.*

Solid state NMR spectroscopy

The main advantage of solid state NMR spectroscopy is its ability to detect amorphous phases and the possibility to provide structural information. The ^{29}Si MAS NMR spectra of 3 cement samples are presented in Figure 5 with assignment of the bands. A broad signal at the chemical shift range between -79 and -85 ppm is the main feature of the spectra and can be assigned to the Si present in the C-S-H phases. The overlap of the peaks does not permit an unambiguous deconvolution between different spectra arising from Si nuclei in different surroundings but it is known that the spectra of C-S-H phases consists of at least three resonances called Q^1, $Q^2(1Al)$ and Q^2 (Lothenbach et al., 2012 and 2014; Richardson, 1999) that could be identified in Figure 5. Q^1 represents a silicate tetrahedron at the end of the C-S-H chain appearing at -79.1 ppm, $Q^2(1Al)$ represents a SiO_4 chain unit connected to one SiO_4 and one AlO_4 tetrahedron (δ = -82.9 ppm) and Q^2 represents a silicate tetrahedron at the middle of the C-S-H chain (δ = -84.5 ppm, see Figure 5).

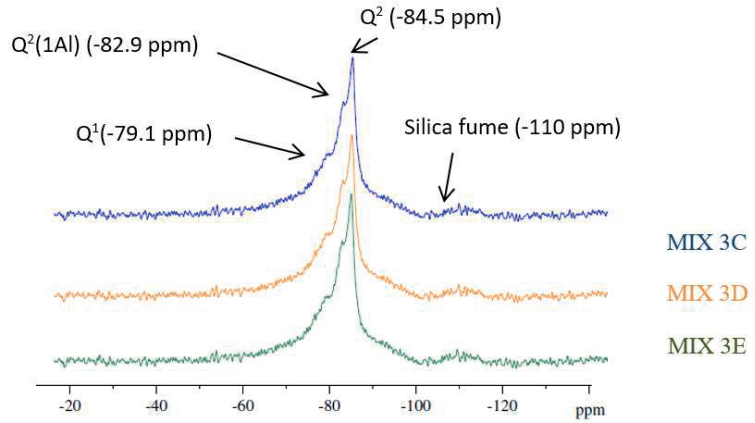

Figure 5: *^{29}Si MAS NMR spectra of hydrated cement (MIX 3C, 3D and 3E) with assignment the chemical shifts.*

The small broad peak at -110 ppm is characteristic for the silica fume which has not reacted during the hydration of the samples (Lothenbach et al., 2012) indicating that only a small amount of Si will be present in this form.

The ^{27}Al-NMR spectra recorded at the three low alkali hardened cement pastes are closely resemble each other presenting all of them two different signals at 58.8 and 13.1 ppm (Figure 6). Al in a tetrahedral coordination environment is generally observed between 50 and 80 ppm, while octahedral Al resonance signals appear between -20 and 20 ppm (Skibsted and Hall, 2008). Figure 6 shows that Al is mainly in an octahedral coordination, and there are only relatively minor amounts of tetrahedral coordinated aluminium. The observed resonances of tetrahedrally ^{27}Al resonances are associated with the aluminum in the nonbridging position of the C-S-H phases and the octahedral ^{27}Al with the presence of ettringite (L'Hôpital et al., 2016).

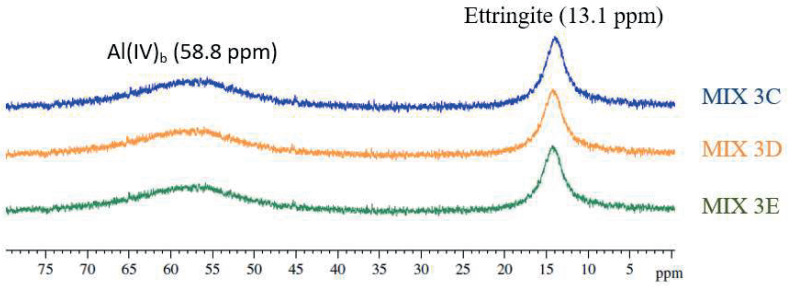

Figure 6: *^{27}Al MAS NMR spectra of hydrated cement (MIX 3C, 3D and 3E) with assignment of the chemical shifts.*

Mercury intrusion porosimetry (MIP) after 90 days of hydration

Various methods can be employed for pore size analyses. Mercury intrusion porosimetry was initially selected for studying the porosity and pore connectivity of the three different cement pastes presented in Ait Mouheb et al. (2017). Three main categories of pores are often described in the literature for cementitious phases: macro, capillary and gel pores (Bajja et al., 2017). As observed in Figure 7, no macro porosity is detected at the samples (> 0.05 μm) and the size of the pores in the hydrated cement phases varies from the micro to the nanoscale. The presence of superplasticizer (mix 3C) eliminates the nano-porosity present in the C-S-H phases (see Figure 7) as observed in Khatib and Mangat (1999).

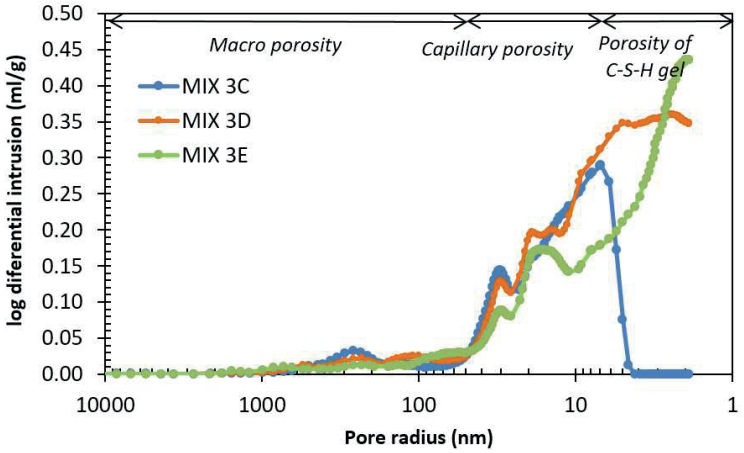

Figure 7: *Pore access at 90 days age of hydrated cement (MIX 3C, 3D and 3E).*

Batch sorption experiments of radiotracers

Sorption values for HTO and sorption mechanism

The results of HTO batch sorption kinetic experiments are shown in Figure 8. The determined R_d value of 0.40 ± 0.13 L/kg and its associated error have been calculated as an average value from all the data obtained from the kinetic sorption experiments. The R_d value for HTO in the three different low pH cement pastes is very weak and independent of the time and the chemistry of the solid indicating that the uptake process presents a similar fast mechanism. In the literature, no R_d values are determined for HTO in low pH cements and lack of sorption data in sulphate-resistant Portland cement (only two sets of experiments) is described in Ochs et al. (2016).

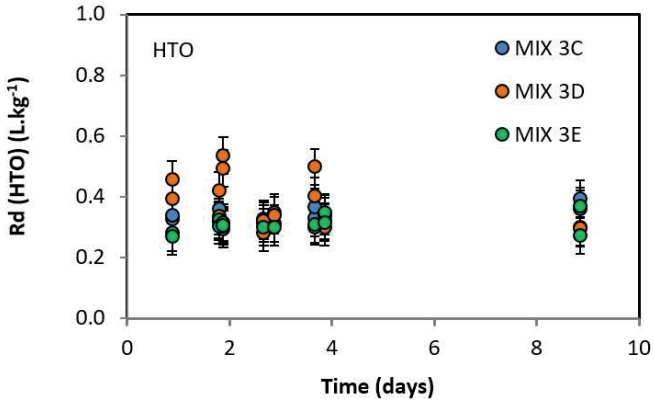

Figure 8: *Sorption of HTO on low pH cement pastes (MIX 3C, 3D and 3E) as a function of time. S/L ratio = 0.133 kg/L. HTO initial concentration = $1.86 \cdot 10^{-9}$ M. Background electrolyte is the one at equilibrium with the low pH cement.*

Comparison of the obtained results with the ones obtained in the literature with other cement pastes (Tits et al., 2003) show that tritium sorption is low in all cases (R_d < 0.8 L/kg). Isotope exchange of HTO with the water bound to the cement has been postulated as possible uptake mechanism (Tits et al., 2003; Ochs et al., 2016). Additionally, Wieland and Van Loon (2002) revealed that higher water / cement ratios can results in higher R_d values for HTO.

In order to demonstrate the postulated mechanism and to derive a comprehensive sorption model, the R_d value has been estimated assuming that HTO and H_2O behave identically and that 100% of the bound water is accessible.

The mass of water bound in three cement samples have been determined experimentally by TG-DSC following the procedure described in Lothenbach et al. (2012) (see previous section *TG - DSC after 90 days of hydratation*). Therefore, the expected R_d will be 0.29 ± 0.03 L/kg which is in agreement with the measured value of 0.3 ± 0.1 L/kg.

Sorption values of $^{36}Cl^-$ and sorption mechanism

The results of $^{36}Cl^-$ batch sorption kinetic experiment are shown in Figure 9. The determined R_d value of 0.22 ± 0.15 L/kg and its associated error have been calculated as an average value from all the data obtained from the kinetic experiments. The R_d value for $^{36}Cl^-$ in the three different low pH cement pastes is very weak and independent of time and chemistry of the solid indicating that the uptake process presents a very similar fast mechanism. In the literature there are not R_d values determined for $^{36}Cl^-$ in low pH cements. However, Ochs et al. (2016) summarized the reviewed R_d values for chloride in different cementitious materials (Nirex reference vault backfill, hardened cement paste, white and grey Portland cement, ordinary Portland cement, sulphate-resisting Portland cement and C-S-H phases) as a function of pH (11.8 - 13.5) for different states of cement degradation. Examination of available data by the authors indicate that the most influential factor on chloride sorption values is the aqueous total chloride concentration, including stable chloride present in cement solid phases and leached into the pores, while pH becomes important only after the effect of total chloride concentration has been accounted for. All available studies (Ochs et al., 2016), indicate a decrease of chloride sorption with increasing total (stable chloride and ^{36}Cl) aqueous concentration. Then, a different chloride behaviour within two concentration ranges has been identified, postulating two different possible uptake mechanism based on experiments performed at pH > 11.8 which are still not well understood (Ochs et al., 2016):

- At Cl^- concentrations lower than few millimolal, $R_d > 10^1$ L/kg is described which might indicative of surface processes (electrostatic interaction and/or anion exchange).
- At Cl^- concentrations above few millimolal, $R_d < 10^1$ L/kg are observed which probably indicate the formation of Friedel´s salt or solid solution with cement phases such as AFm.

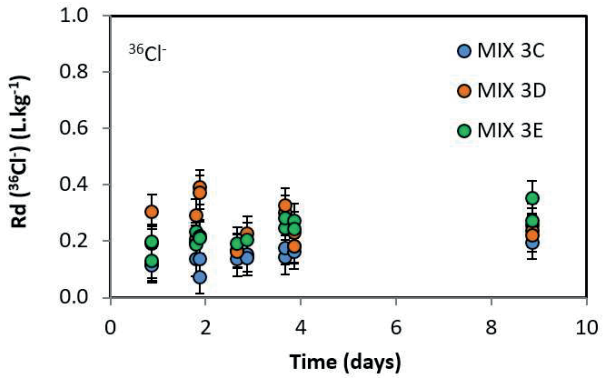

Figure 9: *Sorption of ^{36}Cl on low pH cement pastes (MIX 3C, 3D and 3E) as a function of time. S/L ratio = 0.133 kg/L. Initial total chloride concentration ($^{36}Cl^- = 4.55 \cdot 10^{-6}$ M + $Cl^- = 3.84 \cdot 10^{-3}$ M). Background electrolyte is the one at equilibrium with the low pH cement.*

In the present study, the total concentration of chloride (stable + $^{36}Cl^-$) is equal to $3.8 \cdot 10^{-3}$ M which would indicate the possible formation of solid solutions with Friedel´s salt or ettringite. In order to demonstrate the postulated mechanism and to derive a comprehensive sorption model, the possibility of formation of other phases in the sorption experiments was tested by performing XRD and TG analysis of the solid sample after 30 days of

sorption studies. Formation of other solid phases was not detected by these techniques. At this moment, with the available information, it has been postulated that the uptake process could be associated with surface processes in the C-S-H and C-A-S-H phases identified in the three samples instead of precipitation of secondary phases (Friedel´s salt was not present in the initial cement pastes). In that case zeta potential on cement surfaces could play a significant role for chloride uptake. Available data indicate that sorption of Cl decreases if pH decreases in the range between 12 and 12.5 and are interpreted as being due to the decrease in the zeta potential on cement surfaces. According to Ochs et al. (2016), the zeta potential decreases from pH 12.5 (20 mV) to pH 11 (-10mV) which indicates that the R_d value for Cl would follows the same trend. This mechanism would explain the weak R_d value determined in this work.

The uptake of $^{129}I^-$ and sorption mechanism

The results of $^{129}I^-$ batch sorption kinetic experiment is shown in Figure 10. The determined R_d value of 0.13 ± 0.13 L/kg and its associated error have been calculated as an average value from the data obtained from the kinetic experiments until 10 days. The R_d value for $^{129}I^-$ in the three different low pH cement pastes is very weak, observing almost not sorption. Sorption experiments performed at 25 days indicate a small increase in the sorption which could indicate a slow change of the sorption mechanism which would need to be proved in the future. In the literature (Ochs et al., 2016) there are R_d values determined for $^{129}I^-$ in different cementitious materials (Ordinary Portland cement, concrete, C-S-H phases, AFm and AFt phases) and under different experimental conditions (time, S:L ratio, pH, initial aqueous concentration). Comparison of the obtained results in this work with the ones obtained in the literature using other cementitious materials and calcite indicate that iodine sorption strongly depends on the pH, the Ca:Si ration of the C-S-H phases, the initial I^- aqueous concentration, time and the concentration of other competing anions like Cl^- and sulphate (Ochs et al., 2016). The sorption mechanism of iodine in the 3 studied cements pastes is expected to be similar to the one described for chloride. For this reason, the uptake process for iodine in this study is probably associated with surface processes at the C-S-H and C-A-S-H phases where chlorine competes for sorption sites with chloride (present in higher concentrations).

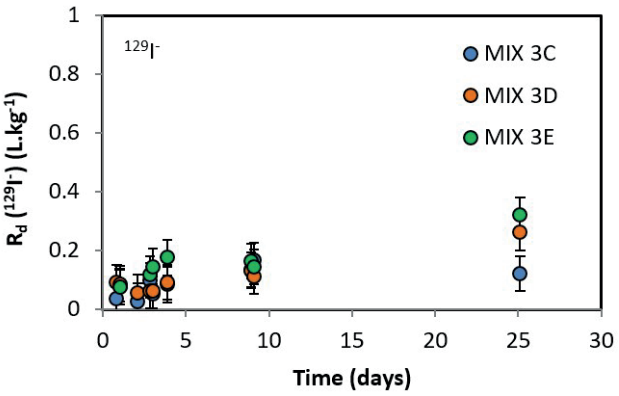

Figure 10: *Sorption of ^{129}I on low pH cement pastes (MIX 3C, 3D and 3E) as a function of time. Total iodine concentration ($I^- + {}^{129}I$) = $5.93 \cdot 10^{-5}$ M.*

Conclusions and Future work

The chemical properties of the 3 low pH cement pastes prepared in this work with Ordinary Portland cement (OPC) and silica fume (40 - 50%) are clearly different from the ones typically found with only OPC. The main hydrated phases formed after 90 days of hydration are the calcium silicate hydrates (C-S-H) with a low Ca/Si ratio

which varies between 0.6 and 0.8 and C-A-S-H phases where a partial substitution of the Si for Al have been produced. The ^{29}Si and ^{27}Al MAS NMR analyses demonstrated the incorporation of aluminium as tetrahedrally coordinated Al(IV) in the bridging position of the C-S-H phases. Unreacted silica fume has also been identified and calcite is present in two of the samples where limestone filler was added. Neither precipitation of strätlingite, katoite nor Friedel´s salt were identified. Additionally, as seen by MIP, the presence of superplasticizer clearly decreases the porosity and the smallest connected pore size detectable of the cement pastes.

Uptake studies of HTO, $^{36}Cl^-$ and $^{129}I^-$ from batch sorption experiments indicate very weak sorption ($K_d < 0.40 \pm 0.13$ L/kg) for the 3 selected radionuclides. The uptake process of Cl and I is probably associated with surface processes in the C-S-H and C-A-S-H phases with competition for sorption sites, between them. In the case of HTO, isotopic exchange with the interlayer water of the C-S-H and the C-A-S-H seems to be the main uptake process.

Besides the completion of the cement sample characterization with additional techniques (especially the characterization of the pore structure) and the potential of the surface, degradation studies of the low pH cement paste by the bentonite pore water using imaging techniques are in progress.

Acknowledgement

The research leading to these results has received funding from the European Union's European Atomic Energy Community's (Euratom) Horizon 2020 Programme (NFRP-2014/2015) under grant agreement, 662147 – Cebama.

Additionally, we would like to acknowledge the colleagues from KIT-INE: Nicolas Finck for the XRD advise, Stefanie Hilpp and Sylvia Moisei-Rabung for the IC and ICP-OES analyses, Tanja Kisely for the TIC, Stephanie Heck, Martina Schlieker, Elke Bohnert and Claudia Joseph for the lab assistance and advise. We thank Francis Claret (BRGM), for his comments and suggestions which have contributed to improve this paper.

References

Ait Mouheb, N., Montoya, V, Borkel, C., Schäfer, T. (2017). Experimental studies on low pH cements / clay interface processes: characterization of low pH cements. Proceedings of the 1st CEBAMA Annual Workshop. KIT Scientific Publishing, KIT-SR 7734.

ANDRA (2005). Andra Research on the Geological Disposal of High-level Long-lived Radioactive Waste - Results and Perspectives. June, 2005.

Bajja, Z., Dridi, W., Darquennes, A., Bennacer, R., Le Bescop, P., Rahim, M. (2017). Influence of slurried silica fume on microstructure and tritiated water diffusivity of cement pastes. Constr. Build. Mater., 132, 85-93.

Beaudoin, J.J., Ramachandran, V.S., Feldman, R.F. (1990). Interaction of chloride and CSH. Cem. Concr. Res., 20, 875-883.

Coumes, C.C.D., Courtois, S., Nectoux, D., Leclercq, S., Bourbon, X. (2006). Formulating a low-alkalinity, high-resistance and low-heat concrete for radioactive waste repositories. Cem. Concr. Res., 36, 2152-2163.

ENRESA (1995). Almacenamiento geológico profundo de residuos radiactivos de alta actividad (AGP). Diseños conceptuales genéricos. Publicación Técnica ENRESA, 11/95.

Khatib, J.M. and Mangat, P.S. (1999). Influence of superplasticizer and curing on porosity and pore structure of cement paste. Cem. Concr. Compos., 21, 431-437.

L'Hôpital, E., Lothenbach, B., Kulik, D.A., Scrivener, K. (2016). Influence of calcium to silica ratio on aluminium uptake in calcium silicate hydrate. Cem. Concr. Res., 85, 111-121.

Lothenbach, B., Le Saout, G., Ben Haha, M., Figi, R., Wieland, E. (2012). Hydration of a low-alkali CEM III/B–SiO_2 cement (LAC). Cem. Concr. Res., 42, 410-423.

Lothenbach, B., Rentsch, D., Wieland, E. (2014). Hydration of a silica fume blended low-alkali shotcrete cement. Phys. Chem. Earth, Parts A/B/C, 70-71, 3-16.

Ochs, M., Mallants, D., Wang, L. (2016). Radionuclide and metal sorption on cement and concrete. Springer.

Richardson, I.G. (1999). The nature of C-S-H in hardened cements. Cem. Concr. Res., 29, 1131-1147.

Skibsted, J. and Hall, C. (2008). Characterization of cement minerals, cements and their reaction products at the atomic and nano scale. Cem. Concr. Res., 38, 205-225.